Earthquake Engineering and Engineering Seismology
Volume 2, Number 2, September 2000, pp. 15-24

Magnitude Scaling of Near Fault Ground Motions

P.G. Somerville [1]

1) *URS Corporation, 566 El Dorado Street, Pasadena, CA 91101, USA, paul_somerville@urscorp.com*

ABSTRACT

The near fault rupture directivity pulse is a narrow band pulse whose period increases with magnitude. Current ground motion models, which all assume monotonically increasing spectral amplitude at all periods with increasing magnitude, do not provide an accurate description of near fault ground motions. The Chi-Chi earthquake was a large magnitude thrust earthquake with a shallow hypocenter and large surface slip. These characteristics may have reduced the damage potential of the intermediate period near fault ground motions caused the Chi-Chi earthquake, compared to strike slip earthquakes and deeper thrust earthquakes of smaller magnitude having buried slip.

RUPTURE DIRECTIVITY EFFECTS IN STRONG GROUND MOTION

An earthquake is a shear dislocation that begins at a point on a fault and spreads at a velocity that is almost as large as the shear wave velocity. The propagation of fault rupture toward a site at a velocity close to the shear wave velocity causes most of the seismic energy from the rupture to arrive in a single large pulse of motion that occurs at the beginning of the record [1,2]. This pulse of motion represents the cumulative effect of almost all of the seismic radiation from the fault. The radiation pattern of the shear dislocation on the fault causes this large pulse of motion to be oriented in the direction perpendicular to the fault, causing the strike-normal ground motions to be larger than the strike-parallel ground motions at periods longer than about 0.5 seconds. To accurately characterize near fault ground motions, it is therefore necessary to specify separate response spectra and time histories for the fault normal and fault parallel components of ground motion.

Forward rupture directivity effects occur when two conditions are met: the rupture front propagates toward the site, and the direction of slip on the fault is aligned with the site. The conditions for generating forward rupture directivity effects are readily met in strike-slip faulting, where the rupture propagates horizontally along strike either unilaterally or bilaterally, and the fault slip direction is oriented horizontally in the direction along the strike of the fault.

However, not all near-fault locations experience forward rupture directivity effects in a given event. Backward directivity effects, which occur when the rupture propagates away from the site, give rise to the opposite effect: long duration motions having low amplitudes at long periods.

The conditions required for forward directivity are also met in dip slip faulting. The alignment of both the rupture direction and the slip direction updip on the fault plane produces rupture directivity effects at sites located around the surface exposure of the fault (or its updip projection if it does not break the surface). Unlike the case for strike-slip faulting, where forward rupture directivity effects occur at all locations along the fault away from the hypocenter, dip slip faulting produces directivity effects on the ground surface that are most concentrated in a limited region updip from the hypocenter.

For this reason, rupture directivity effects in the 1999 Chi-Chi earthquake were confined to a limited region northwest of the hypocenter. Since the hypocenter was fairly shallow, and there may not have been very much slip between the hypocenter and the surface, as suggested in slip models of the earthquake, forward directivity effects in the Chi-Chi earthquake were not very important on average. They are manifested in the single large velocity pulse, strongest on the east (fault normal) component, at some stations such as Tsaotun (TCU075) and Mingchien (TCU129), which are located updip from the hypocenter along the southern part of the fault rupture. Further north, the near-fault ground motion becomes more complex. At the extreme northern end of the fault, the near fault ground motion on the hanging wall side at stations TCU052 (Tanstu) and TCU068 (Shihkang) is dominated by the static ground displacement, and may also be influenced by plastic deformation of the hanging wall, not elastic deformation.

In the near-fault rupture directivity model of Somerville, *et al.* [2], as modified by Abrahamson [3], amplitude variations due to rupture directivity depend on two geometrical parameters. First, the smaller the angle between the direction of rupture propagation and the direction of waves travelling from the fault to the site, the larger the amplitude. Second, the larger the fraction of the fault rupture surface that lies between the hypocenter and the site, up to limit of 40% of the fault length, the larger the amplitude.

MAGNITUDE SCALING OF RESPONSE SPECTRA OF NEAR FAULT GROUND MOTIONS

Strong motion recordings of the recent large earthquakes in Turkey and Taiwan confirm that the near fault pulse is a narrow band pulse whose period increases with magnitude (Fig. 1). The recent earthquakes also have surprisingly weak ground motions at short and intermediate periods (0.1 to 3.0 seconds), weaker than those of smaller (magnitude 6.75 ~ 7.0) earthquakes. These observations require reevaluation of the magnitude scaling in current models of near fault ground motions and in current source scaling relations [4].

On the left side of Fig. 1, rupture directivity pulses of earthquakes in the magnitude range of 6.7 to 7 are compared with pulses from earthquakes in the magnitude range of 7.2 to 7.6. The narrow band nature of these pulses

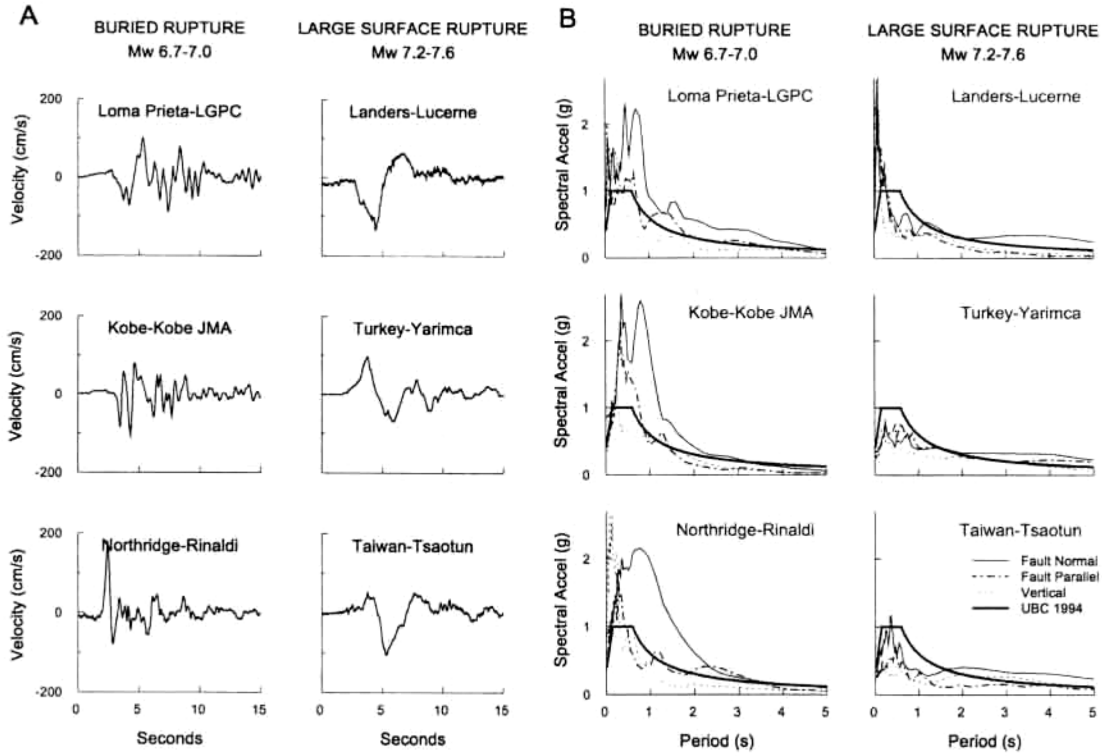

Fig. 1 A: Fault-normal velocity pulses recorded near three moderate magnitude earthquakes (left column) and three large magnitude earthquakes (right column), shown on the same scales. B: Corresponding acceleration response spectra, with 1994 UBC code spectrum shown for reference

causes their elastic response spectra to have peaks, as shown on the right side of Fig. 1. The fault normal components (which contain the directivity pulse) are shown as solid lines, and the fault parallel components, which as expected are much smaller at long periods, are shown by long dashed lines. The 1994 UBC spectrum for soil site conditions is used as a reference model for comparison. The spectra for the large earthquakes (right column) are compatible with the UBC code spectrum in the intermediate period range, between 0.5 and 2.5 seconds, but have a bump at a period of about 4 seconds where they significantly exceed the UBC code spectrum. The spectra of the smaller earthquakes (left column) are very different from those of the larger earthquakes. Their spectra are much larger than the UBC code spectrum in the intermediate period range of 0.5 ~ 2.5sec, but are similar to the UBC spectrum at longer periods.

These features are seen even more clearly in Figs. 2 and 3, which show the velocity and displacement response spectra of the same time histories. The magnitude scaling exhibited in the data in Figs. 1 through 3 is contrary to all current models of earthquake source spectral scaling and ground motion spectral scaling with magnitude, including Somerville, *et al.* [2], which assume that spectral amplitudes increase monotonically at all periods. However, these magnitude scaling

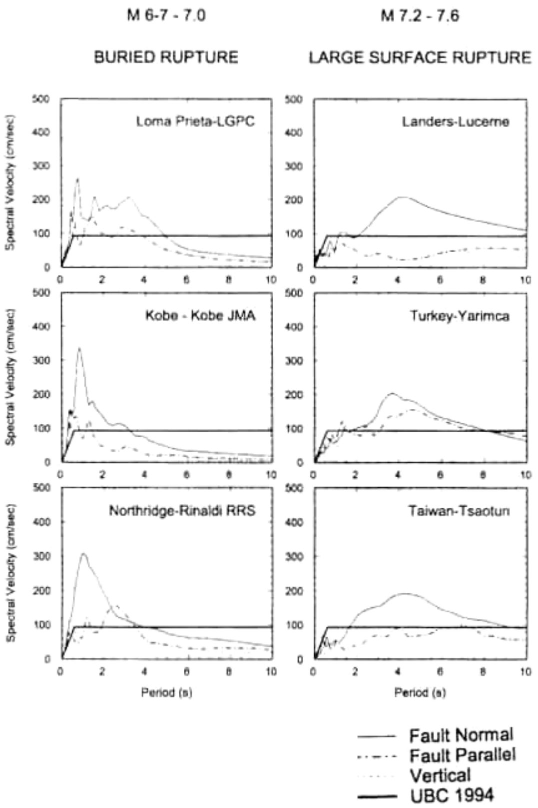

Fig. 2 Spectral velocity of fault-normal pulses of moderate (left) and large (right) earthquakes

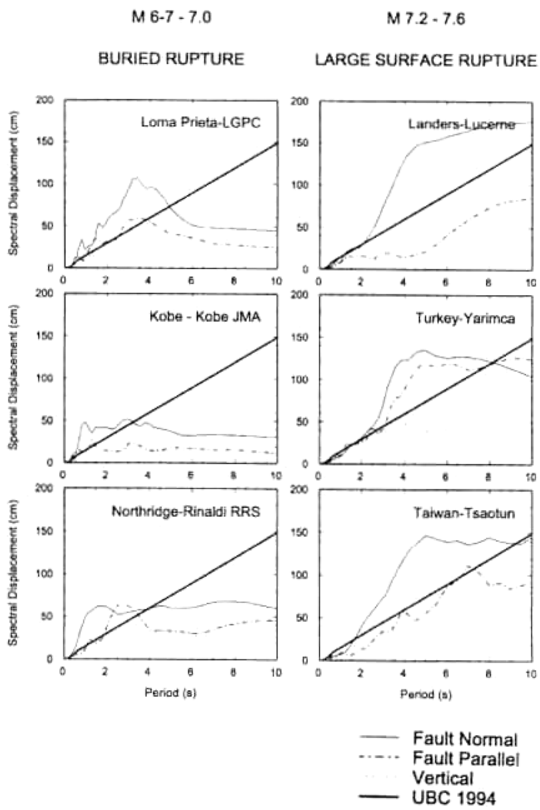

Fig. 3 Spectral displacement of fault-normal pulses of moderate (left) and large (right) earthquakes

features are the natural consequence of the narrow band character of the forward rupture directivity pulse. Near fault ground motions cannot be adequately described by uniform scaling of a fixed response spectral shape, because the shape of the intermediate and long period part of the response changes as the level of the spectrum increases and as the magnitude increases.

GROUND MOTIONS FROM SURFACE AND SUBSURFACE FAULTING

The rupture of the 1989 Loma Prieta and 1994 Northridge earthquakes stopped at depths of several km below the surface. Although there was some surface faulting on Awaji Island during the 1995 Kobe earthquake, the strong motion recordings of the Kobe event were dominated by subsurface faulting on the Suwa and Sumayama faults. Thus all of the earthquakes in the magnitude range of 6.7 ~ 7.0 shown in Figs. 1 though 3 are characterized by subsurface faulting, while all of the earthquakes in the magnitude range of 7.2 to 7.6 are characterized by large amounts of surface faulting. Consequently, some of the differences seen in these figures may be attributable not only to magnitude effects, but to the effects of buried faulting. Indeed, at short and intermediate periods, the ground motions from earthquakes that produce large surface rupture appear to be systematically weaker than those whose rupture is confined to the subsurface, although current empirical ground motion models do not distinguish between these different categories of earthquakes.

This is indicated in Fig. 4, which shows the residuals between the ground motions of selected individual earthquakes, averaged over recording stations, and the empirical ground motion model of Abrahamson and Silva [3] for surface rupture earthquakes (top and center) and subsurface rupture earthquakes (bottom). The zero line represents the Abrahamson and Silva [3] model, which takes account of magnitude, distance, and site conditions, and lines above the zero line indicate an event exceeding the model. At periods shorter than 3 seconds, the ground motions from earthquakes that produce large surface rupture are significantly weaker that those in which rupture is confined to the subsurface.

In the past decade, much progress has been made in the dynamic modeling of fault rupture processes, which may provide insights into why the ground motions from the recent Taiwan and Turkey earthquakes are weaker than expected. In particular, recent work that addresses the dynamic fluid friction aspects of earthquake faulting may explain the difference in ground motions between surface and subsurface faulting. Brodsky and Kanamori [5] propose a model which may not only explain slip weakening, leading to a transition from confined to runaway rupture [6], but may also explain how slip weakening may reduce ground motions at short and intermediate periods, making the

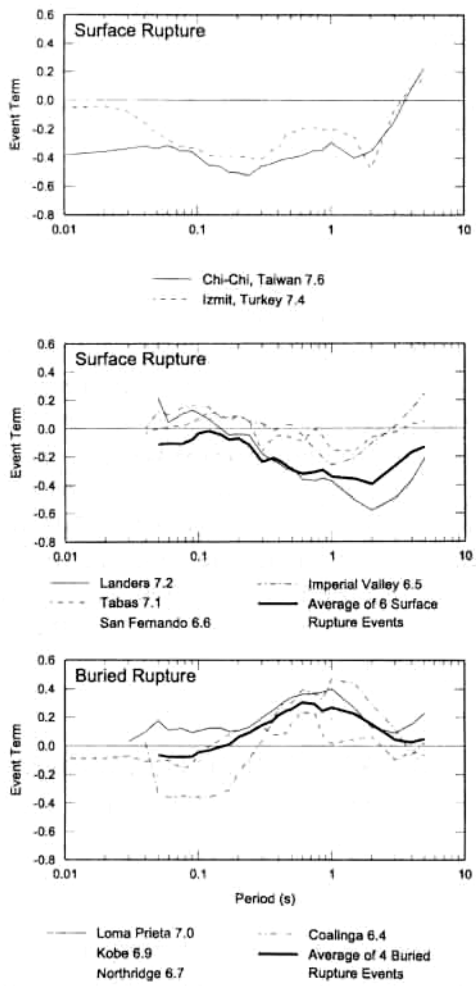

Fig. 4 Comparison of the response spectral amplitude of individual earthquakes, averaged over recording sites, with the amplitude of the average earthquake as represented by the model of Abrahamson and Silva [3], shown as the zero line, which accounts for the magnitude, closest distance and site category. The event terms (residuals) are shown as the natural logarithm of the event/model ratio: +0.2 indicates event exceeding the model by a factor of 1.22, and –0.2 indicates event at 0.82 of model value

rupture directivity pulse narrow band. They show that once slip on the fault has exceeded a critical threshold value, the elevated fluid dynamic pressure generated by faulting between two subparallel surfaces elastically deforms the wall rock, reducing the normal stresses and associated friction across the gap. Analysis of this elasto-hydrodynamic lubrication process using the Sommerfeld number (lubrication pressure normalized by the lithostatic load) predicts a decrease in high frequency radiation once the critical slip distance, which is on the order of a few meters, has been exceeded. This may explain the moderate ground motion levels recorded in the 1999 Turkey and Taiwan earthquakes, show in Figs. 1 through 4.

RELATIONSHIP BETWEEN MAGNITUDE AND PULSE PERIOD

Somerville [7], Somerville, *et al.* [8] and Alavi and Krawinkler [9] developed equations relating the period and amplitude of the near fault pulse period to earthquake magnitude and distance. In Fig. 5, we show a revised relationship between the period of the pulse and earthquake magnitude M_w that has been updated to include data from the 1999 Turkey and Taiwan earthquakes. This relationship uses the period of the largest cycle of the fault normal velocity waveform recorded at stations near the fault that experience forward rupture directivity. The recordings used are within 10km of the fault, and the period is assumed to be independent of the distance from the fault. The only recording of the Chi-Chi earthquake that was used in the revised relationship is the recording from Tsaotun (TCU075), because it is the only recording that shows clear forward rupture directivity effects as discussed above. The data are consistent with a self-similar scaling relationship in which the period of the pulse T_p increases in proportion to the fault length:

$$\mathbf{Log}_{10}\, T_p = -3.1 + 0.5 M_w$$

REPRESENTATION OF NEAR FAULT PULSES FOR INELASTIC STRUCTURAL RESPONSE ANALYSIS

Alavi and Krawinkler [9] proposed that equations like the one given above can be directly used in the design of structures to withstand near fault ground motions, using simple pulse representations of near fault ground motions. One of these pulses, the P_2 pulse, consists of a single cycle of ground velocity that is represented by a triangular pulse. Alavi and Krawinkler [9] show the elastic single degree of freedom (fundamental mode) response spectrum of the P_2 pulse for a magnitude 7 earthquake and a series of inelastic response spectra assuming various values of ductility ratio. The inelastic response spectra were obtained by nonlinear time domain analyses of the response of the structure using the pulse input. Accounting explicitly for multiple degree of freedom (higher mode) effects, Alavi and Krawinkler [9] obtained the inelastic base shear strength demand for a range of maximum story ductility demand values. If the pulse period T_p and the effective acceleration of the pulse that represent the near fault ground motion are known from equations like the one shown in Fig. 5, then this relationship can be used directly for seismic design. The use of simple pulses in place of recorded time histories has the potential to greatly simplify the specification of ground motion time histories for use in structural response analyses.

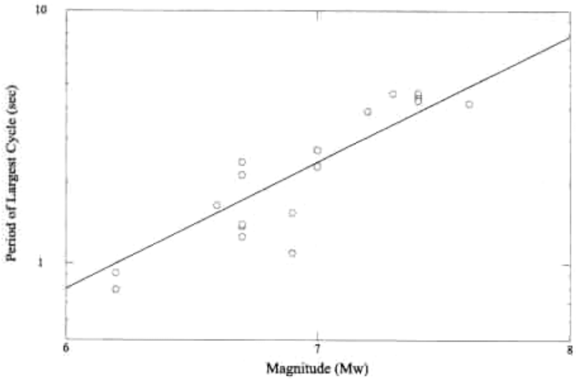

Fig. 5 Relation between period of fault normal pulse and M_w for forward directivity

Elastic response spectra of pulses derived from the model of Alavi and Krawinkler [9] for 3km distance for magnitudes ranging from 6 to 7.5 are shown at the top of Fig. 6. A notable feature of these spectra is that for short periods (less than 1 second), they are stronger for the smaller magnitudes than for the larger magnitudes. The same feature is evident in the data shown in Fig. 1, in which the response spectra for the events in the magnitude range 6.7 to 7.0 are much stronger than for the events in the magnitude range 7.2 to 7.6 for periods less than 3 seconds. The response spectra of the data have a more pronounced peak at the period of the pulse than do the response spectra of the P_2 pulse, indicating the need to improve upon the P_2 model as a representation of the near fault pulse.

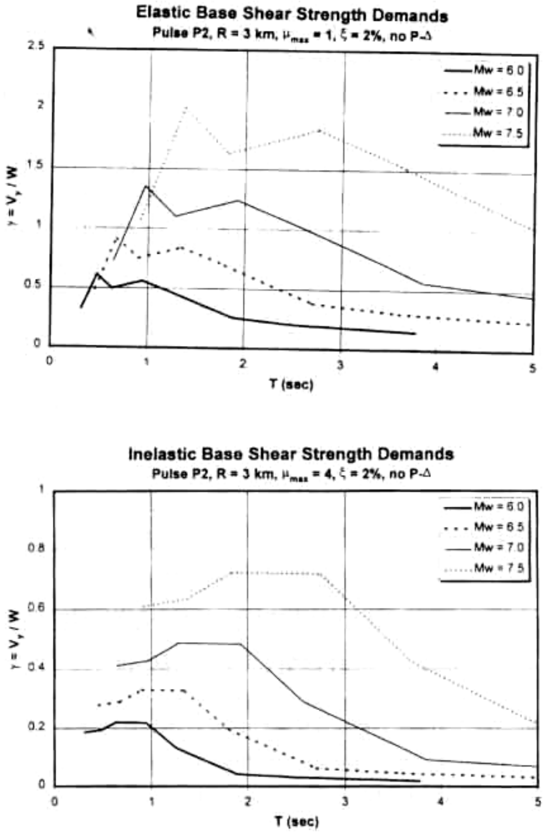

Fig. 6 Elastic (top) and inelastic (bottom, ductility ratio = 4) response spectra of P_2 pulses at 3km distance for four earthquake magnitudes. Source; Krawinkler, 2000

The bottom of Fig. 6 shows the corresponding inelastic response spectra for pulse P_2 for a ductility of 4 for the various magnitudes, obtained by nonlinear time domain analyses of the response of the structure using the pulse input. Unlike the elastic response spectra, for which the short period amplitude is weaker for larger earthquakes, the inelastic response spectrum of larger earthquakes is stronger at all periods than that of smaller earthquakes. This demonstrates a serious shortcoming in the code approach for representing inelastic effects from near fault ground motions. The simple scaling of an elastic code spectrum to produce an inelastic spectrum does not take account of the dramatic change in the shape of the response spectrum as ductility demand increases. This change in shape, reflecting nonlinear effects, indicates the need to specify near fault ground motions in the time domain, not as elastic response spectra, in seismic design codes.

IMPLICATIONS OF NEAR FAULT GROUND MOTION CHARACTERISTICS FOR SEISMIC DESIGN

Since the 1999 Chi-Chi earthquake was a very large earthquake, we may be tempted to assume that the strong ground motions produced by this earthquake are among the largest to be expected from crustal earthquakes in Taiwan. However, the information described above shows that this assumption may be incorrect and significantly unconservative, because the Chi-Chi earthquake was a large magnitude thrust earthquake with a shallow hypocenter and large surface slip. We will show that all of these characteristics reduced the damage potential of the ground motions caused the Chi-Chi earthquake.

First, because of its shallow hypocenter, small amount of slip updip from the hypocenter, and its thrust fault mechanism, the Chi-Chi earthquake did not produce strong forward rupture directivity effects except in a small region updip from the hypocenter. If the hypocenter had been deeper and had been located below a region of large slip (as occurred in the 1994 Northridge earthquake), then much more severe rupture directivity effects would have occurred. Also, rupture directivity effects in strike-slip faulting have the potential to be much more widespread and more severe than those from thrust faulting, because rupture directivity will occur along the entire length of the fault except near the epicenter. The potential for rupture directivity therefore depends on the presence of major strike-slip faults and on the potential for thrust or reverse faulting with deep hypocenters. If it is concluded that the western foothills region of Taiwan is characterized by relatively shallow thrust faulting due to its tectonic environment, the potential for forward rupture directivity effects there may not be so high, but it may be high in other regions having strike-slip faulting or deeper thrust faulting.

Second, we have shown that ground motions from earthquakes that do not rupture the surface may be large than those from earthquakes that produce large surface rupture. This implies that earthquakes having subsurface rupture may cause stronger ground motions than those recorded in the 1999 Chi-Chi earthquake, which produced large surface rupture.

Third, we have shown that the period of the near fault rupture directivity pulse increases with earthquake magnitude. The period of the pulse recorded at Tsaotun during the 1999 Chi-Chi earthquake was about 4 seconds, which is much longer than the natural period of most structures. If the Chi-Chi earthquake had a magnitude of 7 instead of 7.6, it may have produced a forward rupture directivity pulse with a period of about 1.5 to 2 seconds, like those of the 1989 Loma Prieta, 1994 Northridge and

1995 Kobe earthquakes. The ground motions from such a magnitude 7 earthquake may have been more damaging to midrise structures having natural periods in this range than was the actual Chi-Chi earthquake, although that may not be true in light of the inelastic response spectra of Fig. 6.

Near-fault ground motions contain permanent displacements, termed "fling step", due to the static displacement field of the earthquake, as demonstrated in recordings of the 1999 Turkey and Taiwan earthquakes. The static displacement field is distinct from (and not generally correlated with) the dynamic "directivity pulse" effect. For engineering analysis and design, it is therefore necessary to model the static displacement field and rupture directivity effects separately, and then specify them separately or combine them as appropriate for the particular engineering analysis that is done.

To fully represent near-fault ground motions for seismic design, it is necessary to develop separate response spectra for the fault normal and fault parallel horizontal components. In developing ground motion time histories to represent these response spectra, it is important to use the distinct fault-normal and fault-parallel components of recorded or simulated time histories, and apply them in the appropriate orientation when analyzing structural response.

This paper addresses only intermediate period near fault ground motions, which are strongly influenced by rupture directivity effects. At shorter periods (less than about 1 second), hanging wall effects are much stronger than rupture directivity effects. Hanging wall effects (including rock/soil site differences) caused the ground motions to be twice as strong on the hanging wall as on the foot wall for periods less than 1 sec in the Chi-Chi earthquake.

REFERENCES

1. Archuleta, R.J. and Hartzell, S.H. (1981). "Effects of fault finiteness on near-source ground motion," *Bull. Seism. Soc. Am.*, Vol. 71, pp. 939–957.
2. Somerville, P.G., Smith, N.F., Graves, R.W. and Abrahamson, N.A. (1997). "Modification of empirical strong ground motion attenuation relations to include the amplitude and duration effects of rupture directivity," *Seismological Research Letters* 68, pp. 199–222.
3. Abrahamson, N.A. and Silva, W.J. (1997). "Empirical response spectral attenuation relations for shallow crustal earthquakes," *Seismological Research Letters* 68, pp. 94–127.
4. Somerville, P.G., Irikura, K., Graves, R., Sawada, S., Wald, D., Anbrahamson, N., Iwasaki, Y., Kagawa, T., Smith, N. and Kowada, A. (1999). "Characterizing crustal earthquake slip models for the prediction of strong ground motion," *Seismological Research Letters* 70, pp. 59–80.
5. Brodsky, E. and Kanamori, H. (2000). "The elastohydrodynamic lubrication of faults," unpublished manuscript.
6. Kanamori, H. and Heaton, T.H. (2000). "Microscopic and macroscopic physics of earthquakes," *AGU Monograph*, in press.
7. Somerville, P.G. (1998). "Development of an improved representation of near fault ground motions," *Proc. of the SMIP98 Seminar on Utilization of Strong Ground Motion Data*, pp. 1–20.
8. Somerville, P.G., Krawinkler, H. and Alavi, B. (2000). "Development of improved ground motion repre-

sentation and design procedures for near-fault ground motions," Final Report to CSMIP Data Utilization Program, Contract No. 1097-601.

9. Alavi, B. and Krawinkler, H. (2000). "Design considerations for near-fault ground motions," *Proceedings of the U.S.-Japan Workshop on the Effects of Near-Fault Earthquake Shaking*, San Francisco, March 20~21.